

Injection of adult neurospheres induces recovery in a chronic model of multiple sclerosis

Stefano Pluchino*, Angelo Quattrini†‡, Elena Brambilla*, Angela Gritti§, Giuliana Salani*, Giorgia Dina†, Rossella Galli§, Ubaldo Del Carro‡, Stefano Amadio‡, Alessandra Bergami*, Roberto Furlan*‡, Giancarlo Comi‡, Angelo L. Vescovi§ & Gianvito Martino*‡

* Neuroimmunology Unit—DIBIT, † Neuropathology Unit, § Stem Cell Research Institute, and ‡ Department of Neurology and Neurophysiology, San Raffaele Hospital, via Olgettina 58, 20132 Milano, Italy

Widespread demyelination and axonal loss are the pathological hallmarks of multiple sclerosis. The multifocal nature of this chronic inflammatory disease of the central nervous system complicates cellular therapy and puts emphasis on both the donor cell origin and the route of cell transplantation. We established syngenic adult neural stem cell cultures and injected them into an animal model of multiple sclerosis—experimental autoimmune encephalomyelitis (EAE) in the mouse—either intravenously or intracerebroventricularly. In both cases, significant numbers of donor cells entered into demyelinating areas of the central nervous system and differentiated into mature brain cells. Within these areas, oligodendrocyte progenitors markedly increased, with many of them being of donor origin and actively remyelinating axons. Furthermore, a significant reduction of astrogliosis and a marked decrease in the extent of demyelination and axonal loss were observed in transplanted animals. The functional impairment caused by EAE was almost abolished in transplanted mice, both clinically and neurophysiologically. Thus, adult neural precursor cells promote multifocal remyelination and functional recovery after intravenous or intrathecal injection in a chronic model of multiple sclerosis.

The permanent neurological impairment typical of chronic inflammatory demyelinating disorders of the central nervous system (CNS), such as multiple sclerosis, is due to the axonal loss resulting from recurrent episodes of immune-mediated demyelination^{1,2}. So far, experimental cell therapy for these disorders has been based mainly on the transplantation of myelin-forming cells, or their precursors, at the site of demyelination^{3–6}. Although such an approach can trigger functional recovery and restore axonal conduction, the limited migration of lineage-restricted, myelin-forming cells through the brain parenchyma highlights the beneficial effect of transplantation to the site of the injury^{7,8}. This raises critical issues regarding the therapeutic use of focal cell transplantation to treat diseases in which multifocal demyelination is the main pathological feature. Such issues are compounded by the poor expansion capacity of myelin-forming cells in culture^{7,8}, which greatly limits their availability and further hampers their prospective application in clinical settings.

Multipotent neural precursors—with the capacity to generate neurons, astroglia and oligodendroglia—are found in the adult brain and possess the critical features of somatic stem cells⁹. They support neurogenesis within restricted areas throughout adulthood, can undergo extensive *in vitro* expansion and, therefore, have been proposed as a renewable source of neural precursors for regenerative transplantation in various CNS diseases^{10,11}.

Here, we investigate the ability of these neural precursors to reach multiple demyelinating areas of the CNS and to ameliorate disease-related, clinical, neurophysiological and pathological signs when injected both intraventricularly or systemically in an experimental model of multiple sclerosis—EAE. Throughout this study, we used cultures of neural stem cells that were established from the periventricular region of the forebrain ventricles of adult C57BL/6 mice, expanded *in vitro*¹², and labelled with a lentiviral vector by which the expression of the *Escherichia coli* β -galactosidase (β -gal) gene (*lacZ*) was directed to the nuclear compartment. Clonal, subcloning and population studies confirmed the functional stability and stem cell composition of these neural precursor preparations (Supplementary Fig. A), as previously described¹³.

Migration and homing

In CNS inflammation, the upregulation of surface cell adhesion molecules in peripheral blood cells is a prerequisite for their interaction with activated ependymal¹⁴ and endothelial cells^{6,15–17} and their crossing of the blood–brain barrier. Thus, we investigated surface adhesion molecule expression in our cultures. Most (>90%) of the cells expressed CD44 and very late antigen (VLA)-4, but not P-selectin glycoprotein ligand (PSGL)-1, L-selectin and leukocyte function-associated antigen (LFA)-1 (Supplementary Fig. A), indicating that the donor cells in our study might have the capacity to actively interact with the blood–brain barrier and to enter the CNS parenchyma.

To investigate the migratory capacities of neural precursors *in vivo*, we injected them into the cisterna magna (intracerebroventricularly, i.c.) or into the blood stream (intravenously, i.v.) of syngenic, untreated C57BL/6 mice as well as in mice that had been pretreated with lipopolysaccharide (LPS; i.v.) or with tumour-necrosis factor- α (TNF- α) and interleukin (IL)-1 β ¹⁷ (i.c.). Both procedures were used to force the opening of the blood–brain barrier, thus mimicking a CNS-restricted inflammatory-like condition similar to that occurring during the early phases of EAE or multiple sclerosis. One day after transplantation, none of the i.v.- or i.c.-injected cells could be detected within the CNS of untreated mice (data not shown). In contrast, numerous donor cells were found within meningeal spaces (Fig. 1a, b) or around post-capillary venules (Fig. 1g, h) in mice pretreated with LPS or TNF- α /IL-1 β , depending on whether neural precursors were injected i.c. or i.v. This finding indicated that donor cells might have the ability to pass through the blood–brain barrier and enter into the CNS under inflammatory conditions.

Next, we expanded our investigation by injecting neural precursors (1×10^6 cells per mouse) into C57BL/6 mice affected by myelin oligodendrocyte glycoprotein (residues 35–55) (MOG(35–55))-induced chronic EAE¹⁸. Neural precursors were transplanted through i.c. or i.v. injection, either before disease onset (for example, 10 days post-immunization (p.i.)), at the onset of the disease (day 15 p.i.), or one week later (day 22 p.i.). Ten days after

transplantation, the donor cells were distributed along the whole anterior–posterior neural axis (neuraxis) exclusively in those mice with EAE that received neural precursors through i.c. or i.v. injection after the onset of the disease. Notably, although i.c.-injected cells were localized mainly within the submeningeal space in close proximity to subpial inflammatory foci (Fig. 1c–f), the i.v.-injected cells were found around post-capillary venules (Fig. 1i), almost exclusively in areas of CNS damage (Fig. 1j, k). At 10 days after transplantation, relatively few cells were found in the CNS parenchyma. Thirty days after injection of neural precursors, many of the donor cells were localized deeply within the brain parenchyma and displayed a marked distribution pattern: most of them were confined within areas of demyelination and axonal loss, and only very few were found in regions within which the myelin architecture was preserved (Fig. 2).

Engraftment and differentiation

Detailed examination of tissues showed that cells derived from the neural precursors were located closely proximal to demyelinated axons or to axons undergoing a process of active remyelination (Fig. 2a–d). Some of these cells were morphologically indistinguishable from endogenous oligodendrocyte progenitors, with their cell membrane being in close contiguity with the myelin sheets of

some of the surrounding remyelinating axons (Fig. 2a–k). As oligodendrocyte progenitors are able to complete a full programme of myelin re-ensheathment¹⁹, the ensuing idea that neural precursors may differentiate into myelin-forming cells was unequivocally confirmed by electron microscopy analysis. Transplanted cells, showing perinuclear β -gal deposits (Fig. 2e, g, j), were found in close contact with axons that were surrounded by poorly compacted myelin sheets (Fig. 2f, i), a well-established morphological hallmark of active remyelination (Supplementary Fig. B).

Neuropathological analysis of the CNS of EAE mice injected with neural precursors revealed an average density of 19.5 ± 1.1 and 22.1 ± 1.1 β -gal⁺ cells mm^{-2} in the brain and 8.6 ± 0.9 and 7.0 ± 1.0 β -gal⁺ cells mm^{-2} in the spinal cord of i.c.- and i.v.-injected mice, respectively. By means of lineage-specific neural markers, we established that a consistent part of the engrafted cells differentiated into platelet-derived growth factor- α (PDGF α) receptor-expressing oligodendrocyte precursors (i.c.-injected mice: 8.1 ± 1.1 and 3.7 ± 0.9 cells mm^{-2} for brain and spinal cord, respectively; i.v.-injected mice: 9.4 ± 1.0 and 5.3 ± 0.7 cells mm^{-2} for brain and spinal cord, respectively) (Fig. 3a, f). The remaining injected cells generated astrocytes (i.c.-injected mice: 1.9 ± 0.4 and 0.2 ± 0.1 cells mm^{-2} for brain and spinal cord; i.v.-injected mice: 2.9 ± 0.5 and 0.1 ± 0.1 cells mm^{-2} for brain and spinal cord)

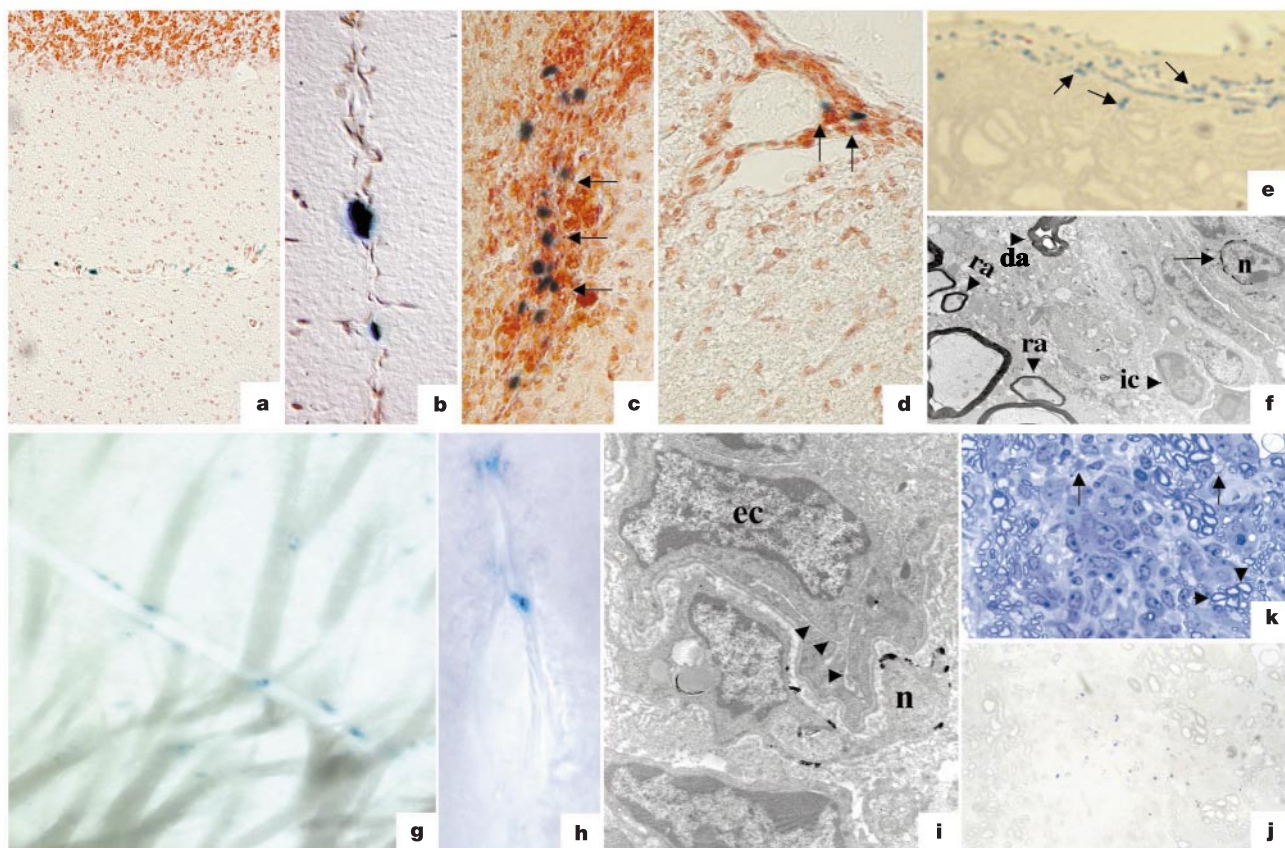


Figure 1 Distribution of *nls-lacZ*-labelled, syngenic neural precursors after i.c. (a–f) and i.v. injection (g–k) in C57BL/6 mice. One day after injection in mice, in which the blood–brain barrier was forced open using pro-inflammatory cytokines¹⁷ (a, b) or LPS¹⁸ (g, h), i.c.-injected neural precursors (blue cells) were located within the meningeal space (a, cerebellum, $\times 20$; b, main sagittal superior scissure, $\times 100$), whereas i.v.-injected neural precursors were confined primarily to perivascular or intravascular areas (g, deep white matter of the lateral ventricles of the brain, $\times 40$; h, white matter of the spinal cord, $\times 40$). Ten days after i.c. injection in EAE mice, neural precursors (arrows) were found both in the brain (c, cerebellum, $\times 40$) and in the spinal cord (d, posterior column, $\times 40$). Furthermore, they were located mainly in the submeningeal space (e, arrows), close to

areas infiltrated by inflammatory cells (ic) containing both remyelinating (ra) and demyelinated axons (f, da, $\times 1,500$). In turn, i.v.-injected neural precursors were found within areas in which clusters of demyelinated (k, arrows, $\times 250$) and normal-appearing axons (k, arrowheads) were visible. i, Neural precursors located across the blood–brain barrier and in close contact with endothelial cells (ec) of the blood–brain barrier were also visible (vascular lumen, arrowheads). Neural precursors are identified by light microscopy (e, $\times 600$; j, $\times 250$) and by electron microscopy (f, $\times 1,500$; i, $\times 6,500$) as cells whose nuclei (n) are surrounded by blue deposits or by rod-shaped electron-dense precipitates (arrows), respectively.

(Fig. 3c) and neurons (i.c.-injected mice: 5.2 ± 0.8 and 2.8 ± 0.6 cells mm^{-2} for brain and spinal cord; i.v.-injected mice: 7.2 ± 1.0 and 4.4 ± 0.7 cells mm^{-2} for brain and spinal cord) (Fig. 3d, e) or retained undifferentiated nestin⁺ morphological features (i.c.-injected mice: 3.0 ± 0.4 and 0.3 ± 0.1 cells mm^{-2}

for brain and spinal cord; i.v.-injected mice: 4.0 ± 0.8 and 0.1 ± 0.1 cells mm^{-2} for brain and spinal cord) (Fig. 3b). Notably, in both i.c.- and i.v.-injected mice, the number of astrocytes derived from neural precursors and that of cells retaining an undifferentiated morphology decreased significantly ($P < 0.005$) in the spinal cord (1.3% astrocytes and 2.5% undifferentiated), as compared with the brain (11.5% astrocytes and 16.8% undifferentiated). Conversely, the number of neural-precursor-derived oligodendrocyte precursors and that of neurons increased in the spinal cord (50.6% oligodendrocyte precursors and 45.6% neurons), as compared with the brain (41.8% oligodendrocyte precursors and 29.8% neurons). A detailed exploration of tissues other than the CNS showed that i.c.- or i.v.-injected neural precursors also reached many of the bodily organs (such as lung, liver, spleen and kidney) within 10 days after transplantation, but could no longer be detected 20 days later (Supplementary Fig. C).

Modulation of growth factor expression

We observed notable changes within the demyelinating areas into which neural precursors had migrated. The typical glia scar surrounding these lesions was consistently and visibly reduced, as indicated by the significant lower density of interleaving astrocyte processes (suggestive of reactive astrogliosis) in demyelinating areas of mice treated i.c. (Fig. 4a) or i.v. (Fig. 4b) with neural precursors, as compared with controls (Fig. 4c). Accordingly, we detected a concomitant decrease in the CNS levels of messenger RNA species

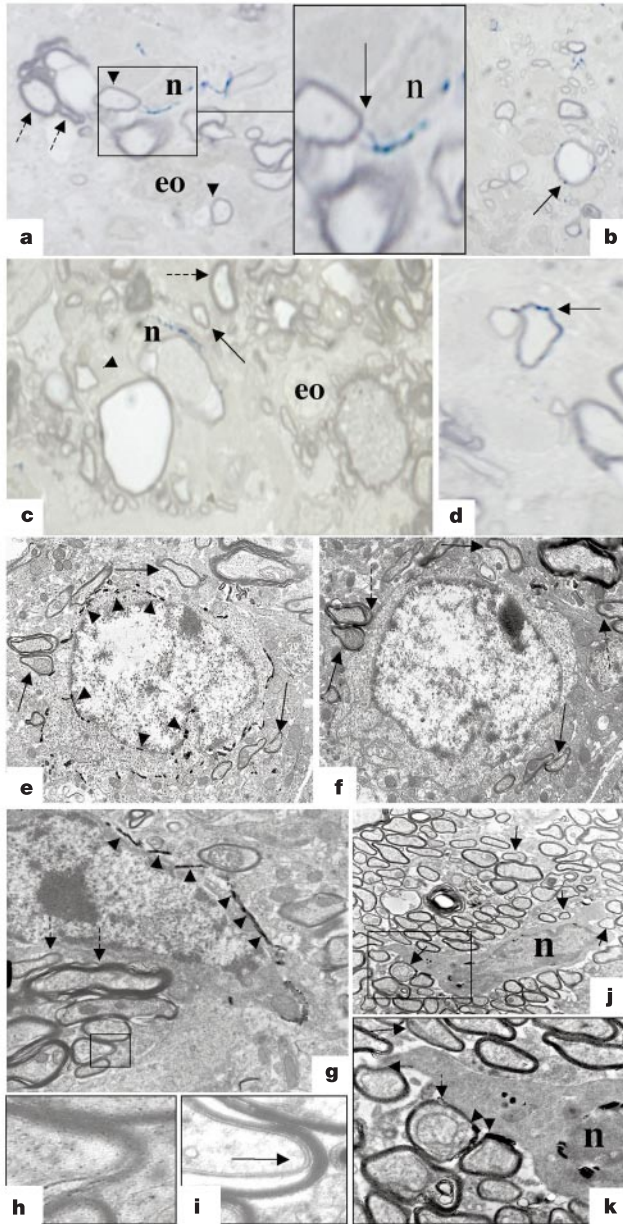


Figure 2 Neural precursors contribute to remyelination of demyelinated axons in EAE mice. **a–d**, Light microscopy showing transplanted neural precursors, the nuclei (n) of which are surrounded by blue deposits, entering into close contact (arrows) with axons surrounded by a larger rim of myelin (dashed arrows) or by a thin rim of myelin (arrowheads). In the same areas, endogenous oligodendrocyte-like cells (eo) coexist. Blue deposits are visible close to myelin lamellae (arrows) (**a, b** and **d**, $\times 600$; **c**, $\times 800$). **e–k**, Electron microscopy showing i.v.-injected β -gal⁺ neural precursors (arrowheads) entering into close contact with various axons and interdigitating within myelin fibres. The cytoplasmic membrane of β -gal⁺ neural precursors contacts several axons surrounded by a thin rim of myelin (arrows). β -gal⁺ dark deposits are also seen close to myelin lamellae (dashed arrows) (**e** and **f**, $\times 3,000$). **g, j**, Axons, which are in close contact with the cell membrane of β -gal⁺ cells (**i**; arrow), are surrounded by poorly compacted, newly formed myelin. **h, i, k**, High-magnification of boxed areas in **g** and **j** (**h** and **i**, $\times 18,000$; **k**, $\times 4,400$).

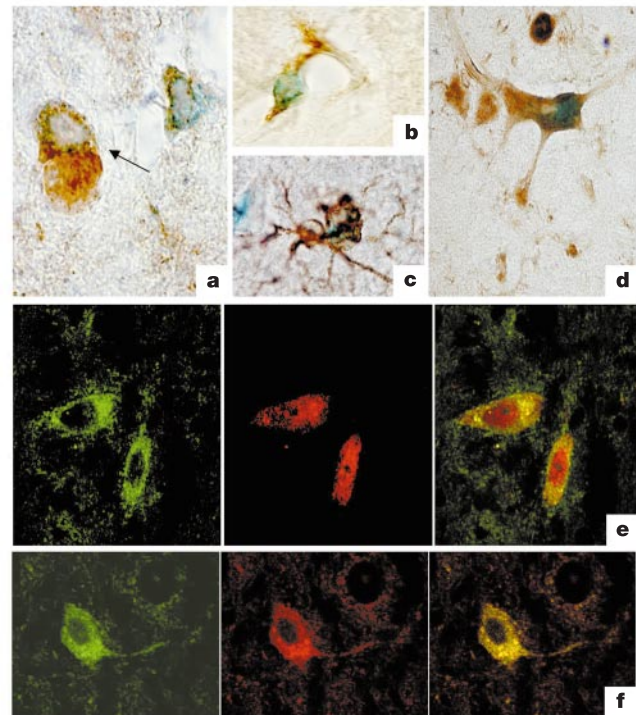


Figure 3 Differentiation of engrafted neural precursors into mature neural cells in EAE mice. **a–d**, Neural-precursor-derived cells (stained blue), which were co-labelled with the oligodendrocyte precursor marker PDGF α receptor, were found within the CNS (arrow) of EAE mice that received either an i.c. or an i.v. injection of neural precursors (**a**, $\times 100$). Within the same area, endogenous unlabelled progenitors were also detected. Blue cells, which were double-labelled with the undifferentiated cell marker nestin (**b**, $\times 100$), the astroglia marker GFAP (**c**, $\times 100$) or the neuronal marker NeuN (**d**, $\times 100$), were also detected. **e, f**, Confocal microscopy showing co-localization of eGFP (green) and the neuronal marker NeuN (**e**, $\times 100$; red) or the oligodendrocyte precursor marker PDGF α receptor (**f**, $\times 100$; red). Engraftment and differentiation of eGFP⁺ neural precursors were comparable to those of β -gal⁺ neural precursors (data not shown).

coding for factors known to drive reactive astrogliosis, such as fibroblast growth factor (FGF)-II²⁰ ($P < 0.05$) and transforming growth factor (TGF)- β ²¹ ($P = 0.06$). Expression levels of mRNA of other neurotrophic growth factors, such as ciliary neurotrophic factor (CNTF), neurotrophin (NT)-3, nerve growth factor (NGF), glial-derived neurotrophic factor (GDNF), brain-derived neurotrophic factor (BDNF) and leukaemia inhibitory factor (LIF), remained unchanged (Fig. 4d). Finally, the overall density of oligodendrocyte progenitors was significantly ($P < 0.001$) increased within demyelinating areas of the spinal cord of mice injected i.c. (27.9 ± 3.9 cells mm^{-2}) (Fig. 4e) or i.v. (25.2 ± 2.3 cells mm^{-2}) (Fig. 4f) with neural precursors, as compared with controls (5.1 ± 0.5 cells mm^{-2}) (Fig. 4g).

Protection from disease progression and recovery

Given the homing of neural precursors into the CNS of EAE mice and the considerable histopathological improvement, we investigated whether their transplantation by the i.c. or i.v. route would also result in clinical recovery in these mice. One week after the onset of the disease (on day 22 p.i.), EAE mice were injected i.c. or i.v. with PBS (hereafter referred to as sham-treated mice), or with equal numbers (1×10^6 cells per mouse) of unsorted syngenic whole bone marrow cells, syngenic fibroblasts or syngenic neural precursors. Moreover, to assess whether transplanted neural precursors might interfere with the ongoing MOG-directed immune response, either working as decoy antigens or by desensitization, dead neural precursors were also injected i.v. into a subgroup of EAE mice. Prominent clinical amelioration was observed exclusively in mice receiving viable neural precursors. Mice receiving neural precursors i.c. began recovering 15 days after cell transplantation (Fig. 5a), whereas i.v.-transplanted mice recovered faster (Fig. 5b), starting 5 days earlier (10 days after cell injection). At the end of the follow-up period (45 days p.i.), both i.c.- and i.v.-treated mice showed a significant recovery from the EAE-related clinical deficits ($P \leq 0.005$ and $P \leq 0.01$, respectively). From a practical perspective, although sham-treated EAE mice were affected by an overt paresis of the hindlimbs, those transplanted with neural precursors displayed clinical features that fell somewhere between the normal behaviour (full recovery) and a minor tail paralysis. Moreover, among the EAE mice completing the follow-up period, 3 of 11 (27%) of those injected i.c. and 4 of 15 (26.6%) of those injected i.v. with neural precursors recovered completely from the disease ($P < 0.05$). None of the mice that received cell types other than neural precursors showed any sign of recovery compared with sham-treated mice (Fig. 5c–e). Clinical recovery was accompanied by a significant decrease in the extent of demyelination ($P < 0.001$) and in axonal loss ($P < 0.01$) 30 days after cell injection (Table 1).

To demonstrate further the functional recovery triggered by injection of neural precursors, we measured central conduction time (CCT) by means of motor-evoked potentials (MEPs) in sham-treated controls and EAE mice treated with neural precursors. CCT is a measure of the time of propagation of the electrical stimulus from motor cortex to spinal motor neurons, with a prolonged or no measurable CCT, indicating slower motor pathways as a consequence of demyelination or axonal damage. Forty-five days p.i., CCT was measurable in all mice, but was significantly ($P \leq 0.05$) reduced in i.c.- (2.97 ± 0.14 ms) and i.v.-treated mice (3.12 ± 0.14 ms) compared with sham-treated controls (3.59 ± 0.18 ms) (Fig. 5f). This positive effect was long lasting. Eighty days after cell transplantation, CCT was measurable in all of the mice injected i.v. (6 mice) or i.c. with neural precursors (9 mice), but in only 4 of 8 (50%) of the sham-treated controls. CCT was closer to normal levels in i.c.- (3.41 ± 0.41 ms) and i.v.-treated mice (3.69 ± 0.49 ms), but it was significantly ($P \leq 0.025$) prolonged in sham-treated controls (4.58 ± 0.89 ms). Doubling either the amount of cells transplanted in each mouse or the number of injections did not result in any increase or quickening in the observed beneficial effects compared with standard injection (1×10^6 cells per mouse) (Supplementary Fig. D).

In vitro modulatory properties

Clinical amelioration in mice injected with neural precursors began 10–15 days after cell transplantation in EAE mice. Because during this time neural precursors and their progeny underwent differentiation, we investigated the basal expression of mRNA species encoding neurotrophic factors in neural precursors and the possible changes that may occur when these cells give rise to their mature neuronal/glia progeny¹². Detectable levels of mRNA for FGF-II, TGF- β , CNTF, GDNF, NGF, BDNF, LIF and NT-3 (Supplementary Fig. E) were found in cultured neural precursors, which were

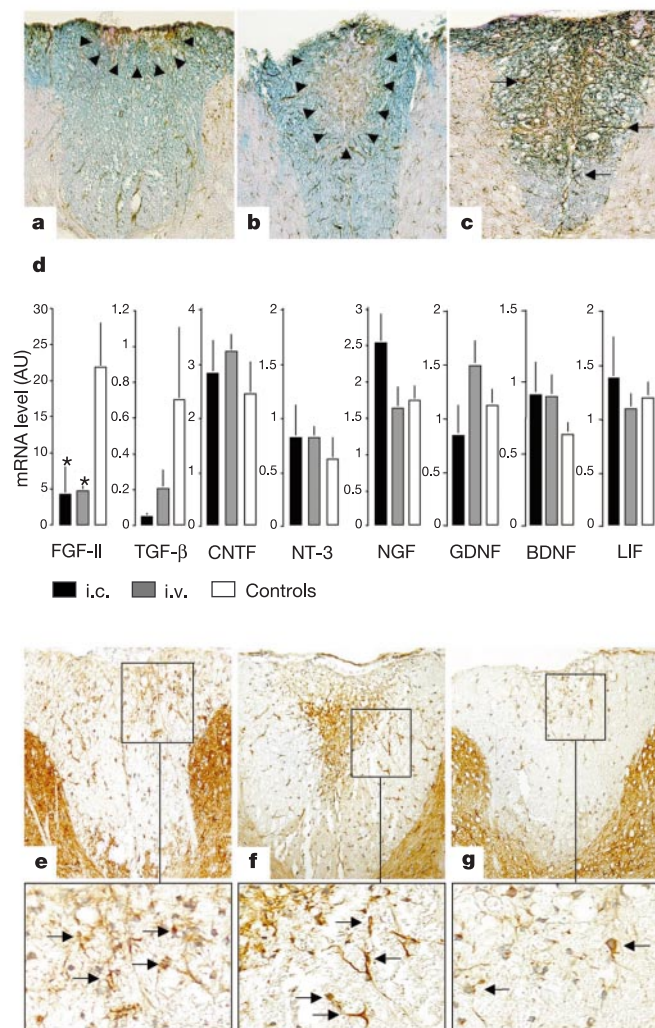


Figure 4 I.c. or i.v. injection of neural precursors into EAE mice reduces glia scarring and modulates neurotrophic growth factor mRNA expression within the CNS. **a–c**, Reduction of reactive astrogliosis occurring within demyelinating areas (arrowheads) in mice injected i.c. (**a**) or i.v. (**b**) with neural precursors, as compared with sham-treated controls (**c**). The blue labelling by Luxol fast staining shows the intact myelin. Interleaving astrocyte processes (arrows; GFAP staining), indicative of reactive astrogliosis, were found in sham-treated but not in neural-precursor-transplanted mice. **d**, mRNA levels of neurotrophic factors in the CNS of sham-treated mice (open bars) and mice injected i.c. (black bars) or i.v. (grey bars) with neural precursors. FGF-II mRNA was significantly (asterisk, $P < 0.05$) reduced in transplanted mice. **e–g**, Increase in PDGFR α receptor-expressing oligodendrocyte progenitors (brown stain) within the posterior columns of the spinal cord of EAE mice transplanted with neural precursors either by i.c. (**e**) or i.v. injection (**f**), as compared with sham-treated animals (**g**). Magnification in **a–c** and **e–g**, $\times 20$.

Table 1 EAE features in C57BL/6 mice treated i.c. or i.v. with neural precursors

Treatment	Route of cell administration	No. of mice	Disease onset (days p.i.)	Maximum clinical score	Cumulative disease score (0–22 p.i.)*	Cumulative disease score (23–45 p.i.)	Inflammatory infiltrates (no. per mm ²)†	Demyelination (% mm ⁻²)‡	Axonal loss (% mm ⁻²)‡
Sham-treated	–	31	14.4 ± 0.6	2.8 ± 0.1	20.5 ± 1.6	49.3 ± 2.1	5.1 ± 0.4	2.6 ± 0.3	3.6 ± 0.5
Neural precursors	i.c.	17	14.1 ± 0.3	2.5 ± 0.1	16.7 ± 1.5	38.4 ± 3.3‡	4.5 ± 0.8	0.7 ± 0.2	1.4 ± 0.3#
Neural precursors	i.v.	22	14.2 ± 0.5	2.6 ± 0.1	17.9 ± 1.4	36.9 ± 3.1§	4.8 ± 0.6	0.6 ± 0.1¶	1.4 ± 0.3☆
Whole bone marrow	i.v.	5	14.0 ± 0.7	2.9 ± 0.3	18.1 ± 1.8	51.9 ± 9.2	6.1 ± 0.5	1.7 ± 0.3	3.8 ± 1.1
Fibroblasts	i.v.	5	15.6 ± 0.6	3.1 ± 0.3	14.1 ± 2.9	54.0 ± 5.6	4.8 ± 0.3	4.1 ± 0.4	4.2 ± 0.6

Data are means ± standard error. i.c., intracerebroventricularly; i.v., intravenously; p.i., post-immunization; whole bone marrow, unsorted whole bone marrow cells. *The cumulative score represents the summation of the single score recorded in each mouse before (from the day of immunization (day 0) to day of cell transplantation (day 22)) and after (from day 23 to day 45 p.i.) cell transplantation.

†Inflammatory infiltrates, demyelination and axonal loss have been quantified on an average of 12 spinal cord sections per mouse for a total of five mice per group.

‡ $P < 0.01$ when compared with sham-treated controls.

§ $P < 0.005$ when compared with sham-treated controls.

|| $P < 0.0001$ when compared with sham-treated controls; $P < 0.0001$ and $P < 0.05$ when compared with fibroblasts injected i.v. and whole bone marrow cells injected i.v., respectively.

¶ $P < 0.0001$ when compared with sham-treated controls; $P < 0.0001$ and $P < 0.01$ when compared with fibroblasts injected i.v. and whole bone marrow cells injected i.v., respectively.

$P = 0.001$ when compared with sham-treated controls; $P < 0.001$ and $P < 0.05$ when compared with fibroblasts injected i.v. and whole bone marrow cells injected i.v., respectively.

☆ $P < 0.01$ when compared with sham-treated controls; $P < 0.01$ when compared with fibroblasts injected i.v.

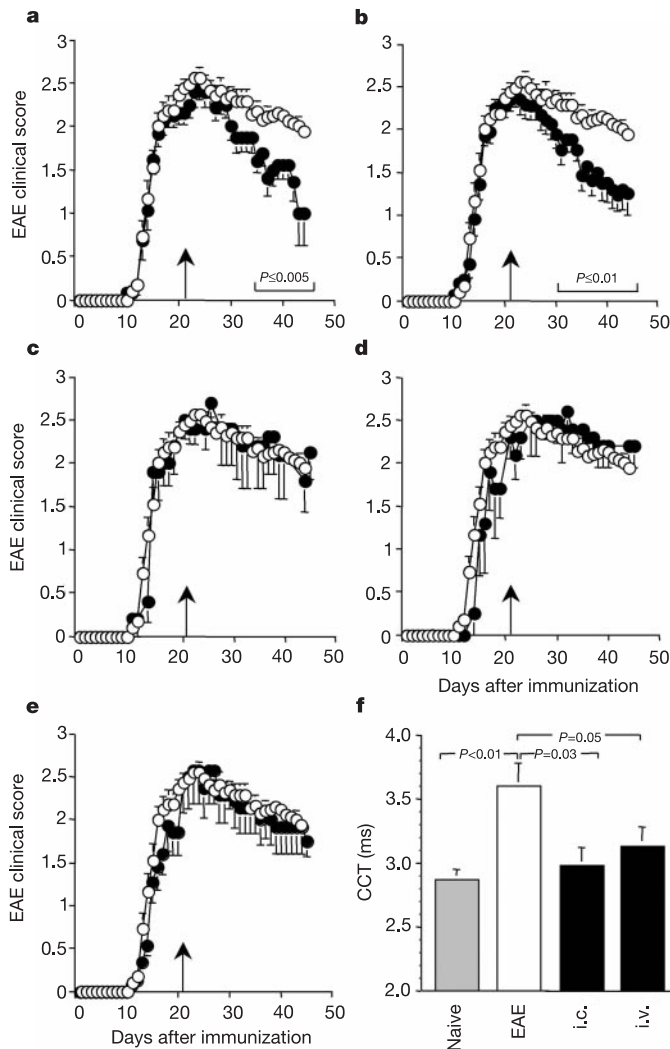


Figure 5 i.v. and i.c. injection of neural precursors after disease onset (arrow) significantly improves clinical features in EAE mice. EAE clinical score (see Methods) in mice injected with different cell types (filled circles) and in sham-treated mice (open circles; $n = 31$). Only the mice that received neural precursors i.c. (**a**, $n = 17$) or i.v. (**b**, $n = 22$) display a pronounced clinical improvement compared with sham-treated mice and mice injected i.v. with unsorted whole bone marrow cells (**c**, $n = 5$), fibroblasts (**d**, $n = 5$) or dead neural precursors (**e**, $n = 7$). **f**, Neurophysiological assessment of myelin conduction

velocity in EAE mice transplanted with neural precursors (i.v., $n = 9$; i.c., $n = 5$), sham-treated EAE mice ($n = 11$) and naive untreated mice ($n = 14$). Significantly ($P \leq 0.05$) lower CCT values, showing improvement of myelin conduction velocity, were recorded in neural-precursor-treated mice when compared with sham-treated animals. Data in the graph are expressed as means (\pm standard error) of at least five different experiments.

unaffected after their differentiation *in vitro*. Notably, CNTF—a factor critically involved in protection from CNS demyelination²²—was fivefold higher in differentiated cells than in neural precursors (Supplementary Fig. E). As the neuroprotective effect of CNTF in EAE²² has been attributed to *in situ* downregulation of TNF- α , we also measured the levels of mRNA for TNF- α both in neural precursors before and after their differentiation *in vitro*, and in the CNS of i.c.- and i.v.-treated EAE mice. Undifferentiated and differentiated neural precursors did not appear to produce TNF- α , which, however, was significantly downregulated in the CNS of mice treated with neural precursors, as compared with controls (Supplementary Fig. E). Accordingly, we also found that the mRNA levels of matrix metalloproteinases (MMP)-2 and -9—two molecules that act synergistically with TNF- α in the breaking of the blood–brain barrier and the facilitation of CNS transport and migration of encephalitogenic lymphocytes in EAE/multiple sclerosis²³—were significantly lower in EAE mice treated with neural precursors, as compared with untreated mice, although the genes *Mmp2* and *Mmp9* were not transcribed in undifferentiated neural precursors and their mature progeny *in vitro* (Supplementary Fig. E).

Bimodal mechanism of action

Our results show that the mechanism underlying the neural-precursor-mediated clinical amelioration is bimodal. First, neural precursors differentiate into myelin-forming cells and establish a programme of anatomical and functional re-ensheathing of myelin at the site of the lesion. Second, in demyelinated areas of mice receiving neural precursor injection, oligodendrocyte progenitors increase by fivefold compared with those in sham-treated controls. Yet, although up to 20% of these derive from donor neural precursors, the remainder are of endogenous origin. Furthermore, astrogliosis—which hampers endogenous axonal remyelination, leading to irreversible axonal loss and functional disability—is greatly reduced in animals transplanted with neural precursors. This shows that, in addition to carrying out direct remyelination, transplanted neural precursors can also act as bystander regulators of endogenous oligodendroglia and of reactive astrogliosis in EAE. Some of the effectors of this ‘humoral’ mechanism may perhaps be molecules that are critically involved in this phenomenon, such as FGF-II and TGF- β ^{20,21}, whose expression is modulated in the CNS after neural precursor transplantation. Nonetheless, it is likely that many other molecules—such as pro-inflammatory cytokines, growth factors (for example, CNTF)²² and/or MMPs²³ that are involved in the effector’s phase of autoimmune demyelination—may also be implicated in this phenomenon.

Cell therapy is a prominent area of investigation in the biomedical field, particularly for the treatment of otherwise incurable neurodegenerative CNS disorders. In this view, both embryonic and neural stem cells are being proposed as an elective source of brain cells for transplantation²⁴. Our findings show that cultures of neural stem cells may function as a therapeutic tool to improve clinicopathological signs and symptoms of chronic inflammatory demyelinating diseases of the adult brain. This reinforces the concept that somatic stem cells may represent an effective ‘weapon’ for the cure of CNS disorders where neurodegeneration causes permanent disability. These findings acquire particular relevance when considering that the pathology studied here is a model of multiple sclerosis, a CNS demyelinating disease of a complex type, presenting us with a particularly difficult challenge. The problems posed by the chronic and inflammatory nature of the disease—through the formation of glia scars and by the depletion of the local pool(s) of oligodendrocyte progenitors that should re-ensheath demyelinated axons^{19,25}—are greatly compounded by the presence of multiple demyelinating plaques diffused throughout the neuraxis. This pathological feature prevents the use of a classical neural transplantation approach, in which the therapeutic cells are injected in the

proximity of the site of the lesion or into its target area, such as in Parkinson’s disease²⁶.

Somatic stem cells can target injured CNS tissue and promote functional recovery^{27,28}. However, cells may promote functional recovery in multiple, diffused areas of the CNS only when injected *in situ* during fetal life²⁹, whereas in adulthood their beneficial effect(s) seem to be achievable only in focal injuries^{11,27–30}. To the best of our knowledge, this work provides the initial evidence showing how neural precursors may represent a renewable source of cells which, when transplanted into the cerebroventricular system or into the blood stream, can reach multiple areas of a chronically injured adult CNS, enter the brain tissue and seek damaged areas where they promote structural and functional recovery. The possibility of injecting therapeutic cells systemically to achieve significant clinical benefit in multiple sclerosis-like syndromes opens new opportunities for the clinical use of stem-cell-based therapies to treat heretofore incurable diseases in humans. □

Methods

Cell preparation and clonogenic analysis

Neural precursor cultures were established and expanded as previously described (see also Supplementary Information)¹². Neural precursors from passage 5 to 10 were used throughout this study. Cells were labelled *in vitro* using a third-generation lentiviral vector pRRLsin.PPT-hCMV engineered with the *E. coli*-derived *lacZ* gene containing a nuclear localization signal (*nls*)³¹. We labelled more than 80% of the cells by this method. Clonal and population studies confirmed the functional stability of the cells used here, as shown previously (see also Supplementary Information)¹³. Whole bone marrow unsorted cells were obtained by flushing femurs and tibiae of 6–8-week-old C57BL/6 mice. Fibroblast cultures were prepared from adult C57BL/6 kidneys dispersed through a 70- μ m cell strainer and maintained in DMEM supplemented with 10% FCS and antibiotics.

EAE induction and treatment

Chronic, relapsing EAE was induced in 122 C57BL/6 mice by subcutaneous immunization with 300 μ l of 200 μ g MOG(35–55) (Multiple Peptide System) in incomplete Freund’s adjuvant containing 8 mg ml⁻¹ *Mycobacterium tuberculosis* (strain H37Ra; Difco). Pertussis toxin (Sigma) (500 ng) was injected on the day of the immunization and again two days later. Body weight and clinical score (0 = healthy; 1 = limp tail; 2 = ataxia and/or paresis of hindlimbs; 3 = paralysis of hindlimbs and/or paresis of forelimbs; 4 = tetraparesis; 5 = moribund or death) were recorded daily. Cells were injected by means of the cisterna magna (i.c.) as previously described¹⁸, whereas i.v. cell injections were performed through the tail vein using a 25-gauge needle. All procedures involving animals were performed according to the guidelines of the Animal Ethical Committee of our Institute.

Histology

Brain, spinal cord and peripheral organs (heart, lung, liver, spleen, gut, kidney) from mice transcardially perfused with PBS followed by 4% paraformaldehyde were removed and processed for light and electron microscopy. Paraffin-embedded tissue sections (5 μ m) were stained with haematoxylin and eosin, Luxol fast blue and Bielschowsky to detect inflammatory infiltrates, demyelination and axonal loss, respectively¹⁸. Quantification of CNS damage was performed using IM–50 image analyser software (Leica) on 300 sections.

To detect the *in vivo* fate of neural precursors in i.v.- and i.c.-injected mice, frozen (10–12 μ m) and fresh agarose-embedded tissue sections (50–80 μ m) were cut and incubated overnight at 37 °C in 5-bromo-4-chloro-3-indolyl- β -D-galactoside (X-gal) solution for nuclear β -gal activity, and processed for immunohistochemistry or counterstained with nuclear red. Sections of CNS showing β -gal⁺ cells were re-cut at 5 μ m and double-stained using anti-glia fibrillary acidic protein (GFAP) for astrocytes (Dako), anti-neuronal nuclear antigen (NeuN) for neurons (Chemicon), anti-PDGFR α receptor for oligodendrocyte progenitors (SantaCruz) and anti-*nestin* (Chemicon) for undifferentiated cells. Appropriate biotin-conjugated (Amersham) secondary antibodies were used. A total of 7,274 double-positive cells were counted on 480 5- μ m sections of CNS (31 brain and 17 spinal cord sections per mouse; five mice per group) taken at 100- μ m intervals. Light and electron microscopy was performed on semi-thin serial sections (1 μ m) from tissues stained with 5-bromo-3-indolyl-beta-D-galactopyranoside, post-fixed in 2% glutaraldehyde and 1% osmium tetroxide, and embedded in Epon as previously described (see also Supplementary Information)³². Confocal microscopy (Bio Rad, MRC 1024) was performed on fresh-frozen brain and spinal cord tissue sections (5 μ m) obtained from EAE mice injected either i.v. (three mice) or i.c. (three mice) with 1 \times 10⁶ of the same neural precursors, transfected with the same lentiviral vector as above but containing the enhanced green fluorescent protein (eGFP) gene in place of the *nls-lacZ* gene³¹. Tissue sections were analysed at 0.5- μ m intervals using the same primary antibodies as above and rhodamine-conjugated secondary antibodies.

Semi-quantitative RT-PCR

Total RNA was extracted from the brain and spinal cord of a minimum of five mice per group and from neural precursors undifferentiated and *in vitro* differentiated for 10 days after growth factor removal, using RNeasy (Molecular System), and complementary

DNA was synthesized. Polymerase chain reaction with reverse transcription (RT-PCR) was performed and PCR products were hybridized with fluorescein-labelled probes. Enhanced chemical fluorescence signal-amplification module (Amersham Pharmacia Biotech) was used; signals were detected using a high-performance laser scanning system (Typhoon 8600, Amersham Pharmacia Biotech). Values were normalized against the *Gapdh* gene and expressed as arbitrary units (AU). Primer and probes have been designed using Primer Express 1.5 software (Applied Biosystem) (see also Supplementary Information).

FACS analysis

Neural precursors were washed and then incubated with fluorescein-isothiocyanate-conjugated anti-mouse CD44, L-selectin, LFA-1, PSGL-1 and VLA-4 antibodies. Isotype control was performed using fluorescein isothiocyanate-labelled mouse control immunoglobulin- γ . Analysis was performed with a FACScan flow cytometer (Becton Dickinson) equipped with CellQuest software, and 50,000 events were acquired.

Neurophysiological assessment

Mice were anaesthetized with tribromoethanol (0.02 ml g⁻¹ of body weight), and placed under a heating lamp to avoid hypothermia. Motor-evoked potentials (MEPs)—muscle responses evoked by transcranial electrical stimulation of the motor cortex—were recorded using a pair of 25-gauge needle electrodes from the contralateral lower limb. The active electrode was inserted into the footpad muscles, whereas the reference was placed subcutaneously between the first and the second digit. The excitatory volleys descending along the cortico-spinal pathways evoke motor potentials in the paw muscles through a trans-synaptic depolarization of alpha motor neurons (cortical MEP). A spinal MEP was also obtained stimulating ventral nerve roots over the lumbar spine, so that a CCT was measured as time difference—expressed in milliseconds (ms)—between cortical and spinal MEP latencies.

Statistical analysis

Data were compared using the Student's *t*-test for unpaired data, the Mann-Whitney *U*-test for non-parametric data, or the χ^2 test.

Received 13 November 2002; accepted 10 March 2003; doi:10.1038/nature01552.

1. Lucchinetti, C. *et al.* Heterogeneity of multiple sclerosis lesions: implications for the pathogenesis of demyelination. *Ann. Neurol.* **47**, 707–717 (2000).
2. Hemmer, B., Archelos, J. J. & Hartung, H. P. New concepts in the immunopathogenesis of multiple sclerosis. *Nature Rev. Neurosci.* **3**, 291–301 (2002).
3. Archer, D. R., Cuddon, P. A., Lipsitz, D. & Duncan, I. D. Myelination of the canine central nervous system by glial cell transplantation: a model for repair of human myelin disease. *Nature Med.* **3**, 54–59 (1997).
4. Groves, A. K. *et al.* Repair of demyelinated lesions by transplantation of purified O-2A progenitor cells. *Nature* **362**, 453–455 (1993).
5. Blakemore, W. F. Remyelination of CNS axons by Schwann cells transplanted from the sciatic nerve. *Nature* **266**, 68–69 (1977).
6. Imaizumi, T., Lankford, K. L., Burton, W. V., Fodor, W. L. & Kocsis, J. D. Xenotransplantation of transgenic pig olfactory ensheathing cells promotes axonal regeneration in rat spinal cord. *Nature Biotechnol.* **18**, 949–953 (2000).
7. Jefferson, S. *et al.* Inhibition of oligodendrocyte precursor motility by oligodendrocyte processes: implications for transplantation-based approaches to multiple sclerosis. *Mult. Scler.* **3**, 162–167 (1997).
8. Franklin, R. J. & Blakemore, W. F. To what extent is oligodendrocyte progenitor migration a limiting factor in the remyelination of multiple sclerosis lesions? *Mult. Scler.* **3**, 84–87 (1997).
9. Clarke, D. & Frisen, J. Differentiation potential of adult stem cells. *Curr. Opin. Genet. Dev.* **11**, 575–580 (2001).
10. Horner, P. J. & Gage, F. H. Regenerating the damaged central nervous system. *Nature* **407**, 963–970 (2000).
11. Teng, Y. D. *et al.* Functional recovery following traumatic spinal cord injury mediated by a unique polymer scaffold seeded with neural stem cells. *Proc. Natl Acad. Sci. USA* **99**, 3024–3029 (2002).
12. Gritti, A. *et al.* Epidermal and fibroblast growth factors behave as mitogenic regulators for a single multipotent stem cell-like population from the subventricular region of the adult mouse forebrain. *J. Neurosci.* **19**, 3287–3297 (1999).

13. Galli, R. *et al.* Emx2 regulates the proliferation of stem cells of the adult mammalian central nervous system. *Development* **129**, 1633–1644 (2002).
14. Deckert-Schluter, M., Schluter, D., Hof, H., Wiestler, O. D. & Lassmann, H. Differential expression of ICAM-1, VCAM-1 and their ligands LFA-1, Mac-1, CD43, VLA-4, and MHC class II antigens in murine *Toxoplasma encephalitis*: a light microscopic and ultrastructural immunohistochemical study. *J. Neuropathol. Exp. Neurol.* **53**, 457–468 (1994).
15. Butcher, E. C. & Picker, L. J. Lymphocyte homing and homeostasis. *Science* **272**, 60–66 (1996).
16. Brocke, S., Piercy, C., Steinman, L., Weissman, I. L. & Veromaa, T. Antibodies to CD44 and integrin $\alpha 4$, but not L-selectin, prevent central nervous system inflammation and experimental encephalomyelitis by blocking secondary leukocyte recruitment. *Proc. Natl Acad. Sci. USA* **96**, 6896–6901 (1999).
17. Del Maschio, A. *et al.* Leukocyte recruitment in the cerebrospinal fluid of mice with experimental meningitis is inhibited by an antibody to junctional adhesion molecule (JAM). *J. Exp. Med.* **190**, 1351–1356 (1999).
18. Furlan, R. *et al.* Intrathecal delivery of IFN- γ protects C57BL/6 mice from chronic-progressive experimental autoimmune encephalomyelitis by increasing apoptosis of central nervous system-infiltrating lymphocytes. *J. Immunol.* **167**, 1821–1829 (2001).
19. Gensert, J. M. & Goldman, J. E. Endogenous progenitors remyelinate demyelinated axons in the adult CNS. *Neuron* **19**, 197–203 (1997).
20. Eclancher, F., Kehrl, P., Labourette, G. & Sensenbrenner, M. Basic fibroblast growth factor (bFGF) injection activates the glial reaction in the injured adult rat brain. *Brain Res.* **737**, 201–214 (1996).
21. Moon, L. D. & Fawcett, J. W. Reduction in CNS scar formation without concomitant increase in axon regeneration following treatment of adult rat brain with a combination of antibodies to TGF β 1 and β 2. *Eur. J. Neurosci.* **14**, 1667–1677 (2001).
22. Linker, R. A. *et al.* CNTF is a major protective factor in demyelinating CNS disease: a neurotrophic cytokine as modulator in neuroinflammation. *Nature Med.* **8**, 620–624 (2002).
23. Alexander, J. S. & Elrod, J. W. Extracellular matrix, junctional integrity and matrix metalloproteinase interactions in endothelial permeability regulation. *J. Anat.* **200**, 561–574 (2002).
24. Temple, S. The development of neural stem cells. *Science* **414**, 112–117 (2001).
25. Franklin, R. J. Why does remyelination fail in multiple sclerosis? *Nature Rev. Neurosci.* **3**, 705–714 (2002).
26. Kim, J. H. *et al.* Dopamine neurons derived from embryonic stem cells function in an animal model of Parkinson's disease. *Nature* **418**, 50–56 (2002).
27. Aboody, K. S. *et al.* Neural stem cells display extensive tropism for pathology in adult brain: evidence from intracranial gliomas. *Proc. Natl Acad. Sci. USA* **97**, 12846–12851 (2000).
28. Choo, M. & Li, Y. Treatment of neural injury with marrow stromal cells. *Lancet Neurol.* **1**, 92–100 (2002).
29. Learish, R. D., Brustle, O., Zhang, S. C. & Duncan, I. D. Intraventricular transplantation of oligodendrocyte progenitors into a fetal myelin mutant results in widespread formation of myelin. *Ann. Neurol.* **46**, 716–722 (1999).
30. Chen, J. *et al.* Therapeutic benefit of intracerebral transplantation of bone marrow stromal cells after cerebral ischemia in rats. *J. Neurol. Sci.* **189**, 49–57 (2001).
31. Follenzi, A., Ailles, L. E., Bakovic, S., Geuna, M. & Naldini, L. Gene transfer by lentiviral vectors is limited by nuclear translocation and rescued by HIV-1 pol sequences. *Nature Genet.* **25**, 217–222 (2000).
32. Feltri, M. L. *et al.* Conditional disruption of beta1 integrin in Schwann cells impedes interactions with axons. *J. Cell. Biol.* **156**, 199–209 (2002).

Supplementary Information accompanies the paper on Nature's website (<http://www.nature.com/nature>).

Acknowledgements We thank L. De Filippis and L. Naldini for providing the lentiviral vectors and G. Constantin and B. Rossi for contributing to FACS analysis. We also thank C. Panzeri for technical help with confocal microscopy. This work was supported by the Italian Multiple Sclerosis Association (AISM), Myelin Project, European Union (EU), Fondazione Agari and BMW Italia.

Competing interests statement The authors declare that they have no competing financial interests.

Correspondence and requests for materials should be addressed to G.M. (e-mail: martino.gianvito@hsr.it) or A.L.V. (e-mail: vescovi@tin.it).